Cell, Vol. 122, 565–578, August 26, 2005, Copyright ©2005 by Elsevier Inc. DOI 10.1016/j.cell.2005.06.016

Systems-Level Dissection of the Cell-Cycle Oscillator: Bypassing Positive Feedback Produces Damped Oscillations

Joseph R. Pomerening,* Sun Young Kim, and James E. Ferrell, Jr.
Department of Molecular Pharmacology
Stanford University School of Medicine
269 West Campus Drive, CCSR 3160
Stanford, California 94305

Summary

The cell-cycle oscillator includes an essential negative-feedback loop: Cdc2 activates the anaphase-promoting complex (APC), which leads to cyclin destruction and Cdc2 inactivation. Under some circumstances, a negative-feedback loop is sufficient to generate sustained oscillations. However, the Cdc2/APC system also includes positive-feedback loops, whose functional importance we now assess. We show that short-circuiting positive feedback makes the oscillations in Cdc2 activity faster, less temporally abrupt, and damped. This compromises the activation of cyclin destruction and interferes with mitotic exit and DNA replication. This work demonstrates a systems-level role for positive-feedback loops in the embryonic cell cycle and provides an example of how oscillations can emerge out of combinations of subcircuits whose individual behaviors are not oscillatory. This work also underscores the fundamental similarity of cell-cycle oscillations in embryos to repetitive action potentials in pacemaker neurons, with both systems relying on a combination of negative and positive-feedback loops.

Introduction

The cell cycles of *Xenopus laevis* embryos provide a particularly striking example of a robust biological oscillator. The cycles of Cdc2 (also termed Cdk1) activation and inactivation in an embryo are rapid and quasisynchronous, with limited embryo-to-embryo variability. In addition, the cycles persist with relatively normal timing and amplitude even when cell-cycle endpoints like DNA replication and spindle assembly are blocked or when embryos are enucleated (Hara et al., 1980). These observations gave rise to the view that the embryonic cell cycle is driven by an autonomous, modular, clock-like regulatory circuit centered on Cdc2 and the anaphase-promoting complex (APC, also termed the cyclosome) (Morgan, 1997; Murray and Kirschner, 1989b). It has been of great interest to try to understand the design principles of the Cdc2/APC oscillator.

In broad outline, the Cdc2/APC network is fairly well understood (Figure 1A). Entry into mitosis is driven by the synthesis and gradual accumulation of cyclin B (Evans et al., 1983; Minshull et al., 1989). In *Xenopus* embryos, the rate of cyclin synthesis establishes the period of the cycle; embryos injected with additional *cyclin B* mRNA cycle faster than control embryos (Hartley et al., 1996). The accumulating cyclin B binds to the cyclin-dependent kinase Cdc2, and, under the proper circumstances, this complex becomes activated and phosphorylates mitotic substrates, driving the transition from interphase to mitosis. The transition from mitosis back to interphase is driven by a negative-feedback loop. Active cyclin B-Cdc2 brings about the activation of the APC, which results in the polyubiquitylation and proteolysis of cyclin (Hershko et al., 1994; King et al., 1995, 1996; Sudakin et al., 1995) (Figure 1A). Although the presence of a negative-feedback loop does not guarantee sustained oscillations of Cdc2 and APC activity, it is difficult to imagine an oscillator that does not contain a negative-feedback loop. Indeed, when APC-resistant cyclin mutants are added to interphase *Xenopus* egg extracts, the extracts approach a steady state of Cdc2 activity rather than oscillating (Murray et al., 1989). This implies that the negative-feedback loop is essential for mitotic oscillations.

In some circumstances, a long negative-feedback loop by itself is sufficient to produce oscillations (Goldbeter, 1991; Goldbeter, 2002). However, the Cdc2/APC system contains additional circuit elements: along with the negative-feedback loop, there is a positive-feedback loop and a double-negative-feedback loop centered on cyclin B-Cdc2 (Figure 1A). Active Cdc2 brings about the phosphorylation and activation of its activator, the phosphatase Cdc25 (Hoffmann et al., 1993; Kumagai and Dunphy, 1992), and active Cdc2 brings about the phosphorylation and inhibition of its inhibitors Wee1 and Myt1 (McGowan and Russell, 1995; Mueller et al., 1995a, 1995b; Tang et al., 1993). These loops could function as a bistable switch (Ferrell, 2002; Novak and Tyson, 1993; Thron, 1996), and recent experimental studies have established that the steady-state response of Cdc2 to constant concentrations of nondegradable cyclin is in fact bistable, with a hysteretic steady-state stimulus/response relationship (Cross et al., 2002; Pomerening et al., 2003; Sha et al., 2003) (see Figure S1 in the Supplemental Data available with this article online). Bistability may ensure that the Cdc2 system cannot rest in a state of intermediate activity. Above a critical concentration of nondegradable cyclin, the system will approach a high-Cdc2-activity, mitotic state; below some other (lower) critical concentration, the system will approach a low-Cdc2-activity, interphase state; and at intermediate cyclin concentrations, the system will approach either the mitotic-like state or the interphase-like state, depending upon the initial conditions, but cannot settle in a state with a partially activated pool of Cdc2. The bistability of Cdc2 activation is believed to help establish discrete M phase and interphase states and to minimize chatter during the transition from interphase to M phase; once M phase has been attained, the system will remain in M phase even if the cyclin concentration dips below the original threshold for M phase entry.

Here we explore the relationship between bistability, which is a steady-state property of the isolated posi-

*Correspondence: pomereni@stanford.edu

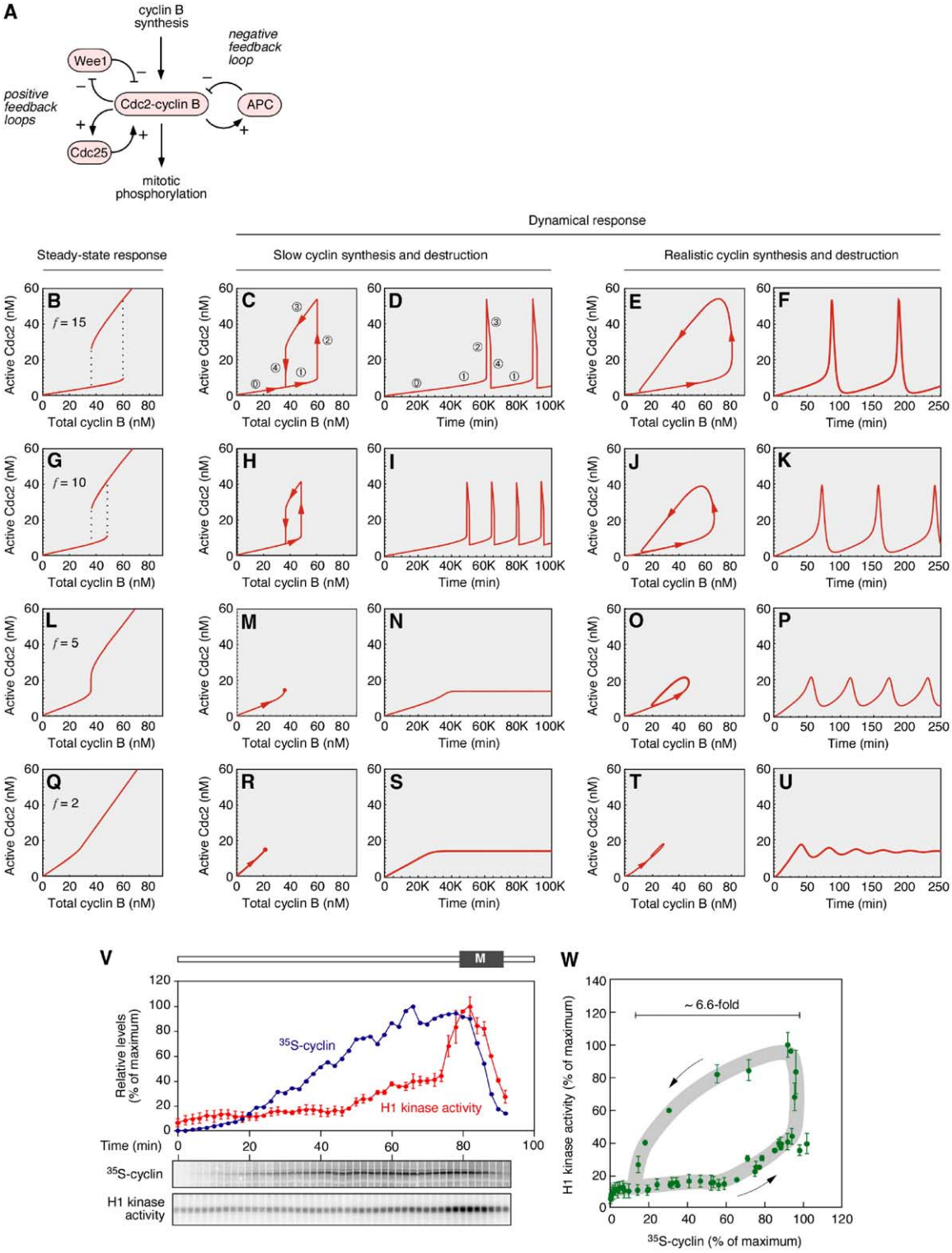

Figure 1. The Connection between Bistable Steady-State Responses and Oscillatory Dynamical Responses

(A) Schematic depiction of the Cdc2/APC system.

(B–U) Computational studies. An ordinary differential equation model of the Cdc2/APC circuit was parameterized to reproduce the experimentally observed steady-state curves for Cdc2 activity as a function of Δ65-cyclin B1 concentration. We calculated steady-state stimulus/response curves and dynamical responses for the model at four different positive-feedback strengths (*f*), where *f* is the ratio of the activities of the active and inactive forms of Cdc25 and Wee1. (B–F) *f* = 15; (G–K) *f* = 10; (L–P) *f* = 5; (Q–U) *f* = 2. Calculated steady-state responses are shown in (B), (G), (L), and (Q). Dynamical responses were calculated for the limiting case of slow cyclin synthesis and destruction (C and D,

tive-feedback loops, and the dynamical properties of the whole Cdc2/APC system. We begin with computational studies, using a reasonably realistic ordinary differential equation model for the Cdc2/APC system, to define the circumstances under which positive feedback is important for oscillations. We then experimentally test the importance of positive feedback through two approaches. First, we supplement cycling *Xenopus* egg extracts with modest concentrations of Cdc2AF. Cdc2AF is not subject to phosphorylation by Wee1 and Myt1 or dephosphorylation by Cdc25 and therefore short-circuits the normal positive-feedback system (Jin et al., 1998; Krek and Nigg, 1991; Norbury et al., 1991). Second, we block the activation of endogenous Cdc2 with a constitutively active form of Wee1 (Wee1-OP11), forcing cycles to be driven solely by Cdc2AF. Our findings support the view that the Cdc2/APC system functions as a relaxation oscillator, or "integrate-and-fire" oscillator, with positive feedback being essential for sustained oscillations.

Results

The Relationship between Bistability and Oscillations

We began by examining the relationship between bistability, which is a steady-state property of one subcircuit of the Cdc2/APC network, and the dynamical properties of the complete Cdc2/APC system. We explored this issue computationally, using an ordinary differential equation model of the Cdc2/APC system. Our model is similar in many ways to the Novak-Tyson model, which was proposed more than a decade ago (Novak and Tyson, 1993) and refined subsequently (Marlovits et al., 1998). The Novak-Tyson model and the one used here differ mainly in the assumed sources of ultrasensitivity. A detailed description of the model can be found in the Supplemental Data.

Our basic approach was to parameterize the model with rate constants and protein concentrations that yielded both bistability (in the modeled steady-state activity of Cdc2 as a function of cyclin concentration in the absence of cyclin degradation) and sustained oscillations (in the modeled dynamical activity of Cdc2 in response to constantly synthesized, degradable cyclin B). We then systematically varied a parameter critical for bistability. For the computations presented here, the parameter chosen was the strength of the feedback from Cdc2 to Wee1 and Cdc25 (denoted *f* in Figures 1B, 1G, 1L, and 1Q). From these computations, we could determine if there was a connection between the presence of a bistable steady-state response and an oscillatory dynamical response.

Initially we assumed that cyclin synthesis and destruction were slow compared to the rates of phosphorylation and dephosphorylation of Cdc2, Wee1, Cdc25, Plx1, and the APC. This assumption is unrealistic, but it simplifies the analysis of the system and provides a starting point for further analysis. Under this assumption, the system should always stay close to the steady-state stimulus/response curve, where the steady-state stimulus/response relationship (Figure 1B) defines the dynamical cyclin/Cdc2 phase plot of the oscillator (Figure 1C). Thus, if the system begins with no cyclin and cyclin synthesis exceeds cyclin destruction (as is true in *Xenopus* egg extracts that are just beginning to cycle), the activity of Cdc2 will climb along the lower curve of the steady-state stimulus/response relationship (Figures 1C and 1D, segments 0 and 1). Once the concentration of cyclin exceeds a threshold, the lower curve disappears and the system snaps to the upper curve (Figures 1C and 1D, segment 2). At this M phase level of Cdc2 activity, we assume that the APC becomes activated and the rate of cyclin destruction exceeds that of cyclin synthesis. The system will progress down the upper curve (Figures 1C and 1D, segment 3) until it reaches the lower threshold, whereupon the system snaps back to the lower curve (Figures 1C and 1D, segment 4) and the second cycle begins (Figures 1C and 1D, segment 1). Thus, in the limit of slow cyclin synthesis and destruction, the oscillations in Cdc2 activity arise because the system travels around a hysteretic stimulus/response curve.

Next we considered what would happen if the positive feedback were weaker. For modest decreases in the feedback strength (*f*), the hysteresis loop becomes smaller (Figure 1G), and the amplitude of the oscillations decreases (Figures 1H and 1I). Once the positive feedback is weakened below some critical level, the bistable, hysteretic stimulus/response relationship collapses into a monostable relationship, and the discontinuities in the stimulus/response curve are lost (Figures 1L and 1Q). At the same critical feedback strength, the oscillations disappear (Figures 1M, 1N, 1R, and 1S). Therefore, in the limit of slow cyclin synthesis and destruction, the connection between bistability in the steady-state responses and oscillations in the dynamical responses is simple: oscillations will be present if and only if bistability is present.

Thus far, we have assumed that cyclin synthesis and destruction are quite slow compared to the phosphorylation and dephosphorylation reactions for Cdc2, Wee1, Cdc25, Plx1, and the APC. In actuality, the timescales

H and I, M and N, R and S) and for a more realistic rate of cyclin synthesis and destruction (E and F, J and K, O and P, T and U). Dynamical responses are shown both as phase plots (C, E, H, J, M, O, R, T) and as time courses (D, F, I, K, N, P, S, U).

(V and W) Experimental studies. The dynamical relationship between cyclin levels and Cdc2 activity was determined by adding [^{35}S]methionine to a cycling *Xenopus* egg extract and removing samples every 2 min to determine relative levels of cyclins (by p13 agarose precipitation) and Cdc2 kinase activity (by histone H1 kinase assay). Additional aliquots were taken every 10 min to assess the morphology of added sperm chromatin by DAPI staining and epifluorescence microscopy.

(V) Time course of morphological changes (single determinations), cyclin levels (single determinations), and H1 kinase activities (duplicate determinations; quantitated data are shown as means ± SEM).

(W) Phase plot of the relationship between cyclin levels and Cdc2 activity. In this representation, the data points lie on a wide loop (drawn in gray).

for the various processes are comparable. As the timescale for cyclin synthesis and destruction becomes increasingly less separable from the timescale of phosphorylation and dephosphorylation, the phase-plane orbit becomes increasingly different from the steady-state stimulus/response curve (see Figure S2). For realistic rates of cyclin synthesis and destruction, the model predicts substantial overshoots and undershoots in the orbit of the system around the steady-state hysteresis loop (Figure 1E). These include an overshoot of segment 2 since an appreciable amount of cyclin will be synthesized while the system switches toward the upper curve, an undershoot of segment 3 since some cyclin destruction will occur as the system approaches the mitotic leg of the stimulus/response curve, and an overshoot of segment 4 because cyclin destruction will continue while Cdc2 and the APC switch off. The exact size and shape of the phase-plane orbit depend upon the particular response functions and kinetic parameters assumed in the model. However, the general prediction of overshoots and undershoots is quite robust. The overshoots and undershoots correspond to phase shifts in the relationship between Cdc2 activity and APC activity, and they add a sort of momentum that can allow the Cdc2/APC system to oscillate in the absence of bistability. This is illustrated in Figures 1L, 1O, and 1P. At this assumed level of feedback strength (f = 5), the steady-state response is monostable but still highly ultrasensitive. The system does not oscillate in the limit of slow cyclin synthesis and destruction (Figures 1M and 1N), but it does oscillate for more realistic rates of cyclin synthesis and destruction (Figures 1O and 1P). Thus, the requirement for bistability is relaxed here. Lowering the feedback strength even further (f = 2) changes the sustained oscillations into a damped approach to a stable steady state (Figures 1Q, 1T, and 1U) even at realistic rates of cyclin synthesis and destruction. Note that the exact feedback strength at which the transition from sustained to damped oscillations occurs depends upon the parameters (rate constants and concentrations) assumed for the model. Indeed, it is possible to choose parameters that permit oscillations in the absence of positive feedback (data not shown).

In summary, in the limit of slow cyclin synthesis and destruction, bistability is strictly required for oscillations. At more realistic rates of cyclin synthesis and destruction, this requirement is relaxed; phase delays in the negative-feedback loop may allow the Cdc2/APC system to oscillate in the absence of a bistable steady-state response (compare Figures 1N and 1P). Conversely, positive feedback may allow the system to oscillate when the phase delays in the negative feedback alone would not (compare Figures 1P and 1U).

Experimental Determination of the Cdc2-Cyclin Phase Plot

To test these concepts and determine how important positive feedback is for oscillations in cycling *Xenopus* egg extracts, we experimentally determined how closely the oscillator's orbit in the Cdc2-cyclin phase plane corresponded to the previously determined hysteretic steady-state relationship (Pomerening et al., 2003; Sha et al., 2003). Cycling *Xenopus* egg extracts were prepared, [^{35}S]methionine was added to label newly synthesized proteins, and aliquots were taken every 2 min to determine cyclin levels (by p13 agarose precipitation) and Cdc2 activities (by histone H1 kinase assay) over one full cell cycle. As shown in Figure 1V, cyclin levels rose through the first 80 min of the cycle and then fell by 90% over the next 10 min. Cdc2 activity rose gradually for 75 min, rose more sharply over the next 10 min, peaked just after nuclear-envelope breakdown, and then fell by 70% over the next 10 min. These data agree well with less detailed time-course studies from a number of other laboratories (Gabrielli et al., 1992; Minshull et al., 1990; Murray and Kirschner, 1989a; Solomon et al., 1990).

Plotting these same data in the phase-plane representation showed that the cycle of cyclin synthesis/destruction and Cdc2 activation/inactivation defines a large loop (Figure 1W). The cyclin concentration on the right side of the loop was about 6.6-fold higher than that on the left side of the loop (Figure 1W). This is substantially larger than the difference between the on threshold and off threshold in the steady-state stimulus/response relationship, which was never greater than a factor of 2 or 3 (Figure S1 and Pomerening et al., 2003; Sha et al., 2003). Thus, the orbit of the dynamic cyclin/Cdc2 system appears to be substantially wider than the steady-state hysteresis loop, with significant overshoots. The observed orbit is in reasonable agreement with modeled orbits (Figures 1E and 1J), which suggests that both positive feedback (which could ensure oscillations even at low rates of cyclin synthesis) and phase delays in the negative feedback (as evinced by the overshoots of the steady-state hysteresis loop) contribute to the robustness of the cell-cycle oscillator. However, the size of the overshoots leaves open the possibility that positive feedback is not essential for Cdc2 oscillations; the system might function as a negative-feedback oscillator (Goldbeter, 1991; Novak and Tyson, 1993), with the positive-feedback loops dispensable for oscillations.

Short-Circuiting the Positive Feedback by the Addition of Cdc2AF

We next sought to determine how important positive feedback is for oscillations in cycling extracts. Our first approach was to supplement extracts with recombinant FLAG-tagged Cdc2AF, which has the two inhibitory phosphorylation sites (Thr14 and Tyr15) changed to nonphosphorylatable residues. These mutations render Cdc2AF impervious to phosphorylation by Wee1 and Myt1, breaking the Cdc2/Wee1/Myt1/Cdc25 positive-feedback loop. Control extracts were supplemented with wild-type recombinant FLAG-Cdc2 (hereafter denoted Cdc2wt). The maximum concentration of exogenous Cdc2wt or Cdc2AF that was practical to add was 200 nM, compared with an estimated concentration of 230 nM for endogenous Cdc2 (data not shown). Assuming that Cdc2wt and Cdc2AF have similar maximal specific activities, the exogenous Cdc2wt or Cdc2AF should increase the maximal level of Cdc2 activity by 87%. We checked this estimate by adding near-saturating concentrations of cyclin (400–500 nM) to control ex-

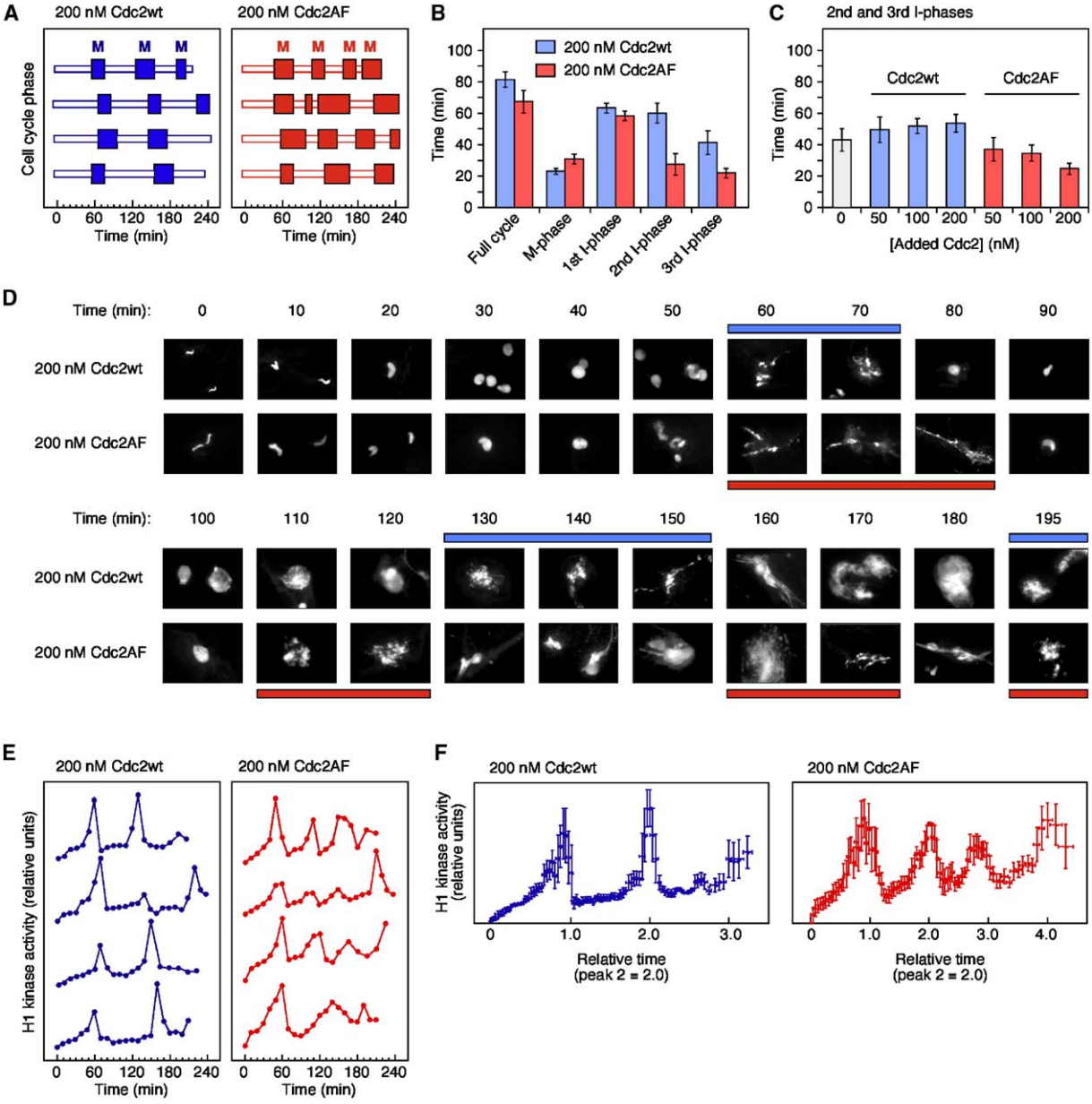

Figure 2. The Effects of Added Cdc2AF on Cell-Cycle Dynamics

(A) Time course of mitotic entry and exit, as assessed by DAPI staining and epifluroescence microscopy of added sperm chromatin, for extracts treated with either 200 nM Cdc2wt or 200 nM Cdc2AF. Data are taken from four independent experiments.

(B) Timing of cell-cycle phases. Data are taken from four independent experiments and are expressed as means ± SEM.

(C) Dose dependence. Extracts were treated with 0, 50, 100, or 200 nM Cdc2wt or Cdc2AF. The duration of the second and third interphases is plotted. Data are taken from four independent experiments for the buffer-treated extracts, two independent experiments for the 50 nM Cdc2wt/Cdc2AF-treated extracts, two independent experiments for the 100 nM Cdc2wt/Cdc2AF-treated extracts, and four independent experiments for the 200 nM Cdc2wt/Cdc2AF-treated extracts. Data are shown as means ± SEM.

(D) Sperm-chromatin morphology. Sperm chromatin was added to extracts; aliquots were taken at various times and stained with DAPI. Sperm chromatin is initially hypercondensed. Over the first 20 min, the chromatin decondenses and forms interphase nuclei. The nuclei then periodically undergo mitosis, as indicated by chromatin condensation and nuclear-envelope breakdown. Time points scored as mitotic are denoted by the bars above or below the photomicrographs. These photomicrographs correspond to experiment 1 (top) in (A) and (E).

(E) Time course of histone H1 kinase activities for extracts treated with 200 nM Cdc2wt or 200 nM Cdc2AF. Data are taken from four independent experiments.

(F) Pooled H1 kinase data. The time courses from individual experiments were rescaled to make the second peak of Cdc2 activation occur at t = 2.0 units. The rescaled data were taken together and expressed as running averages, with four data points per average. Data are plotted as means ± SEM.

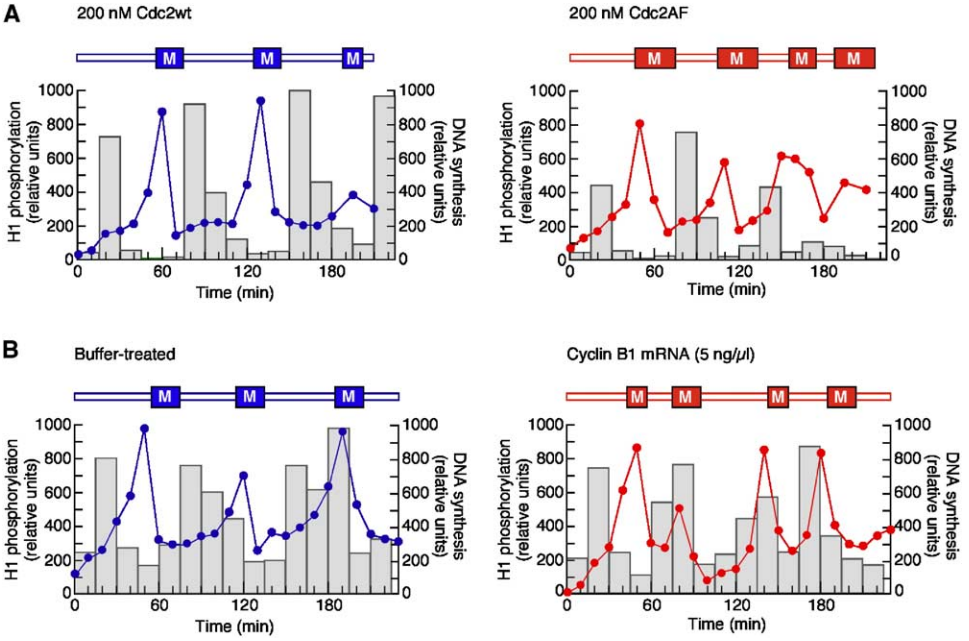

Figure 3. DNA Replication in Cycling Extracts Accelerated by Cdc2AF or Cyclin B1

(A) Sperm-chromatin morphology, histone H1 kinase activity, and DNA replication in extracts treated with 200 nM Cdc2wt or 200 nM Cdc2AF.
(B) Sperm-chromatin morphology, histone H1 kinase activity, and DNA replication in extracts treated with buffer or *cyclin B1* mRNA (5 ng/μl).

tracts or extracts supplemented with 200 nM Cdc2wt or Cdc2AF and assessing the resulting steady-state levels of Cdc2 activity. The resulting maximal Cdc2 activities were 50%–90% above those seen with no added Cdc2 (Figure S3), confirming that we were able to achieve a modest perturbation of Cdc2 activity.

This modest perturbation of Cdc2 activity markedly altered the dynamics of cell-cycle progression and Cdc2 oscillations (Figure 2). Despite the inevitable variations from extract to extract (e.g., extract #4 was slower than extract #1; Figures 2A and 2E) and from cycle to cycle (e.g., the second peak of H1 kinase activity appeared to be anomalously low in the 200 nM wt sample of extract #2; Figure 2E), several clear differences between the Cdc2wt- and Cdc2AF-treated extracts were apparent. First, the Cdc2AF-treated extracts cycled more rapidly than the Cdc2wt-treated extracts. A total of 15 rounds of mitosis were observed in the four extracts treated with Cdc2AF versus a total of 10 rounds in the four Cdc2wt-treated extracts (Figure 2A). The overall shortening of the cycles in the Cdc2AF-treated extracts occurred despite a lengthening of M phase (Figure 2B), implying that the interphases were substantially shortened in the CdcAF-treated extracts, particularly the second and third interphases (Figure 2B). The shortening of interphase was dose-dependent: 50 nM and 100 nM Cdc2AF had less effect than 200 nM (Figure 2C).

There were also qualitative differences in nuclear morphology in the Cdc2AF- versus Cdc2wt-treated extracts (Figure 2D). Cdc2wt-treated extracts exhibited distinct, unmistakable interphase periods during which nuclei formed and then enlarged (e.g., Figure 2D, Cdc2wt-treated, 80–120 min). The transitions out of M phase were sometimes more difficult to discern in the Cdc2AF-treated extracts; the newly forming nuclei did not get much chance to coalesce, grow, and smooth out before the next round of mitosis ensued (e.g., Figure 2D, Cdc2AF-treated, 170–195 min).

Next we examined detailed time courses of histone H1 kinase activities in the Cdc2wt- and Cdc2AF-treated extracts. Cdc2 activation was more gradual and less explosive in the Cdc2AF-treated extracts (Figures 2E and 2F). Cdc2 inactivation was also more gradual and less complete (Figures 2E and 2F), suggesting that the dynamics of Cdc2 activation determines the extent of APC activation. Finally, the amplitudes of successive oscillations decreased, with the system damping toward a state of intermediate Cdc2 activity (Figures 2E and 2F). These findings indicate that positive feedback is important for normal sustained cycles of Cdc2 activation and inactivation. These findings also provide a plausible mechanism to explain the cell-cycle acceleration and morphological changes seen in the Cdc2AF-treated extracts.

DNA Synthesis Is Compromised in Cdc2AF-Treated Extracts

Given the shortened interphases in the Cdc2AF-treated extracts, we asked whether the early M phases resulted from accelerated DNA replication or whether DNA replication was being compromised by premature M phases. To address this question, we monitored DNA synthesis in Cdc2wt- and Cdc2AF-treated extracts. The Cdc2wt-treated extracts underwent four strong rounds of DNA synthesis, with each S phase promptly following the completion of the previous M phase (Figure 3A, left panel). The Cdc2AF-treated extracts also underwent

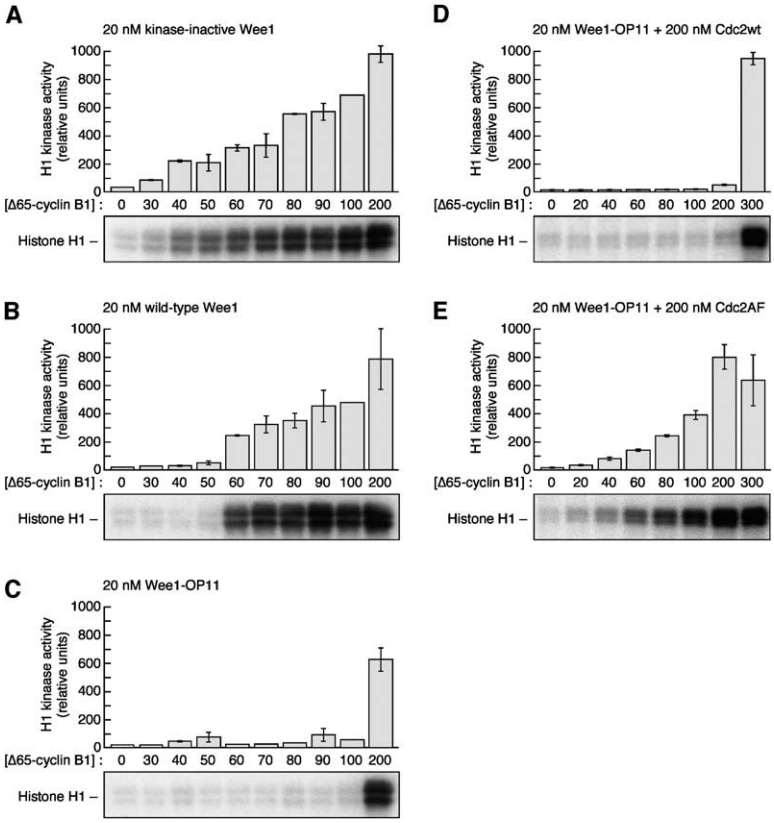

Figure 4. Suppression of Cdc2 Activation by Wee1 and Wee1-OP11

Cycloheximide-treated interphase extracts were treated with various concentrations of Δ65-cyclin B1 in presence of added Wee1 and Cdc2 as indicated. Histone H1 kinase assays were carried out in duplicate. Representative autoradiograms are shown together with phosphorimager-quantitated data expressed as means ± SEM.

four rounds of DNA synthesis, but its extent was diminished, particularly in the third and fourth cycles (Figure 3A, right panel). Thus, the accelerated interphases in the Cdc2AF-treated extracts were due to the altered dynamics of mitotic entry and exit rather than to an accelerated completion of DNA replication.

Accelerating the Cycle with *Cyclin B1* mRNA

To determine whether the damped Cdc2 oscillations and diminished DNA synthesis seen in Cdc2AF-treated extracts were simply due to the rapidity of the cell cycle, we set out to accelerate the cycles without compromising the positive-feedback loops. Injecting cyclin message into the blastomeres of early *Xenopus* embryos is known to accelerate their cleavages (Hartley et al., 1996). We applied a similar approach to extracts. As shown in Figure 3B, the addition of *cyclin B1* mRNA (5 ng/μl) decreased the average cycle length by about 25%, similar to the decreases seen in Cdc2AF-treated extracts (Figure 2). However, there was no apparent damping of Cdc2 oscillations and little effect on DNA synthesis (Figure 3B, right panel) as compared to the buffer-treated control (Figure 3B, left panel). Higher concentrations of *cyclin B1* mRNA drove mitotic entry but prevented mitotic exit (data not shown), as previously reported (Hartley et al., 1996). Taken together, these findings show that Cdc2AF has a more substantial effect on Cdc2 oscillations and DNA synthesis than can be accounted for by the extent of cycle acceleration that it produces.

Strategies for Forcing Extracts to Rely Solely on Cdc2AF

Thus far, we have observed the consequences of short-circuiting positive feedback by adding feedback-resistant Cdc2AF to extracts that still contained endogenous wild-type Cdc2. As a next step, we had hoped to replace the wild-type Cdc2 with Cdc2AF or, as a control, with recombinant Cdc2wt and see if the effects on cycling would be more severe. However, pilot experiments suggested that this depletion/reconstitution approach was impractical. As an alternative, we set out to force the extract to rely exclusively upon added Cdc2AF by neutralizing the endogenous Cdc2 with recombinant Wee1.

Previous work has shown that the addition of Wee1 to cycling *Xenopus* egg extracts delays the activation of endogenous Cdc2 (Mueller et al., 1995a; Walter et al., 2000). Recently we constructed a form of Wee1, denoted Wee1-OP11, that lacks 11 potential sites of mitotic phosphorylation and exhibits an interphase-like high activity in both interphase extracts and M phase extracts (S.Y.K. and J.E.F., unpublished data). We set out to determine whether Wee1-OP11 would be suitable for inhibiting endogenous Cdc2, forcing the extract to rely upon added Cdc2AF.

We added kinase-minus Wee1, wild-type Wee1, or constitutively active Wee1-OP11 at approximately physiological concentrations (20 nM; Mueller et al., 1995a; Walter et al., 2000) to cycloheximide-treated interphase extracts. We next added various concentrations of recombinant Δ65-cyclin B1 (a nondegradable form of

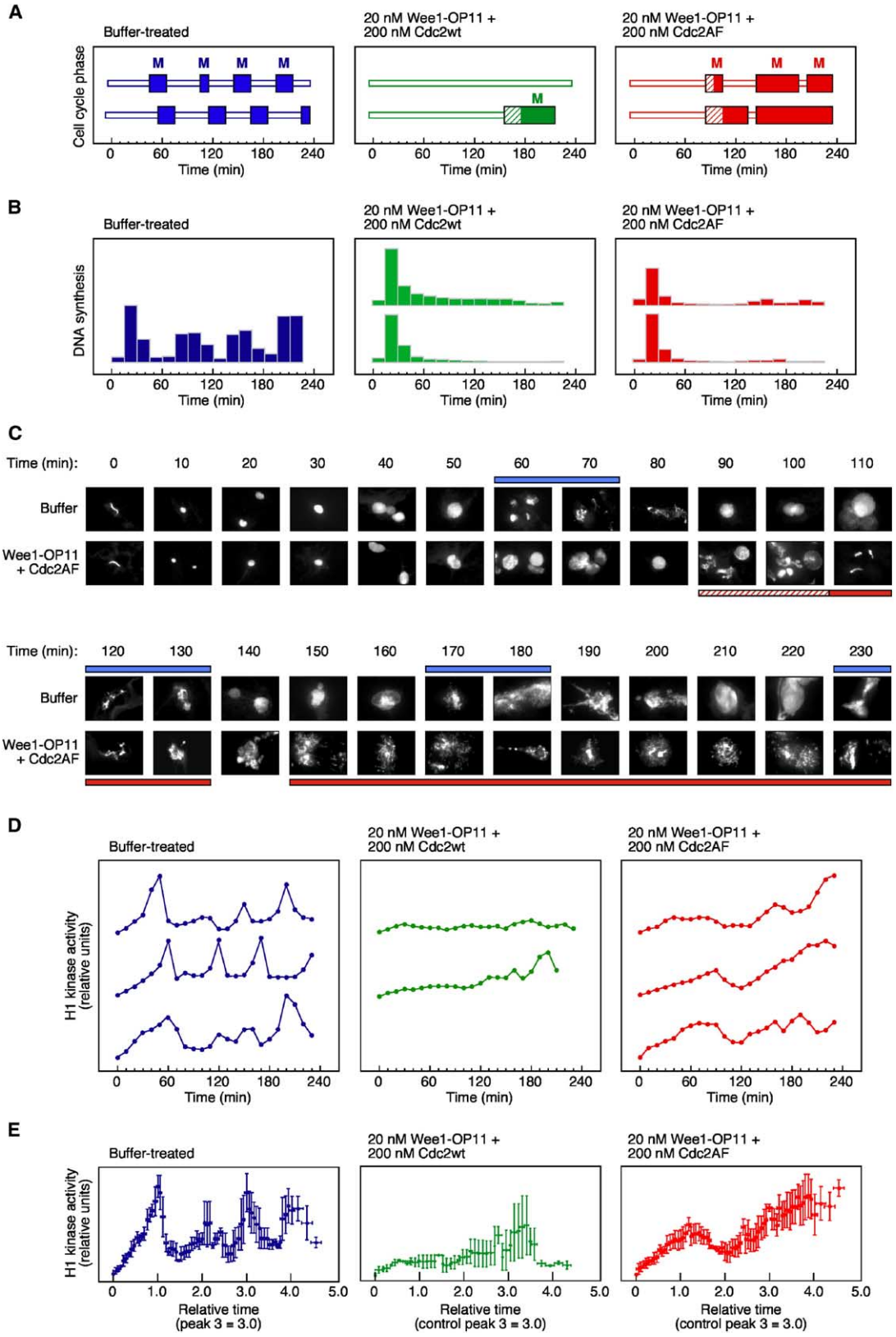

Figure 5. The Effects of Added Cdc2AF and Wee1-OP11 on Cell-Cycle Dynamics

(A) Time course of mitotic entry and exit, as assessed by DAPI staining and epifluorescence microscopy of added sperm chromatin, for extracts treated with buffer (left), 200 nM Cdc2wt plus 20 nM Wee1-OP11 (middle), or 200 nM Cdc2AF plus 20 nM Wee1-OP11 (right). The hatched bars denote time points that contained both interphase and M phase nuclei. Data are taken from two independent experiments.

cyclin B1), let the extracts approach a steady state, and assessed the resulting levels of Cdc2 activity. In the extract treated with kinase-minus Wee1, the threshold for activating Cdc2 was approximately 40 nM Δ65-cyclin B1 (Figure 4A). In the extract treated with wild-type Wee1, the threshold increased to 60 nM Δ65-cyclin B1 (Figure 4B). Finally, in the Wee1-OP11-treated extract, the required concentration of Δ65-cyclin B1 was greater than 100 nM (Figure 4C). From this, we inferred that 20 nM Wee1-OP11 should be sufficient to substantially delay the activation of wild-type Cdc2 in cycling extracts.

In addition, we added combinations of 20 nM Wee1-OP11 and either 200 nM Cdc2wt or 200 nM Cdc2AF to cycloheximide-treated interphase extracts, added various concentrations of recombinant Δ65-cyclin B1, let the extracts approach a steady state, and then assessed the resulting levels of Cdc2 activity. The activation of Cdc2 was found to be highly switch-like in extracts treated with Wee1-OP11 plus Cdc2wt (Figure 4D) and much more graded in extracts treated with Wee1-OP11 plus Cdc2AF (Figure 4E). This is consistent with the idea that the combination of Wee1-OP11 and Cdc2AF forces the extract to run off a version of Cdc2 that responds in a graded fashion and thus does not exhibit bistable responses.

Accordingly, we set out to compare the dynamics of extracts treated with Wee1-OP11 (20 nM) and Cdc2AF (200 nM) to those of control extracts and extracts treated with Wee1-OP11 (20 nM) and Cdc2wt (200 nM). Control extracts cycled normally, with four rounds of mitosis (Figure 5A, left) and peaks of H1 kinase activity (Figures 5D and 5E, left) alternating with four rounds of DNA synthesis (Figure 5B, left). In extracts treated with Cdc2wt and Wee1-OP11, mitosis and H1 kinase activation were blocked (experiment 1) or substantially delayed (experiment 2) (Figures 5A, 5D, and 5E, middle), and there was only the initial round of DNA synthesis (Figure 5B, middle). Replacing the Cdc2wt with Cdc2AF allowed the Wee1-OP11-treated extracts to cycle (Figure 5A, right); however, the cycles were quantitatively and qualitatively abnormal. The onset of the first mitosis was delayed relative to buffer-treated extracts (Figure 5A left and right and Figure 5C). This delay was probably due to the fact that more than 50% of the newly synthesized cyclin B would form complexes with endogenous Cdc2 that could not be further activated due to the presence of Wee1-OP11, while less than 50% of the newly synthesized cyclin B would form activatable complexes with Cdc2AF. Mitotic entry was also more gradual and more variable from nucleus to nucleus in the Cdc2AF+Wee1-OP11-treated extracts, with two time points showing coexisting interphase and M phase nuclei (Figures 5A and 5C). The measured Cdc2 activities reflected a gradual entry into M phase as well; Cdc2 activities gradually rose over the first 60–90 min of incubation, and there was no explosive peak of Cdc2 activation (Figures 5D and 5E, right). Following this gradual rise, Cdc2 activity gradually decreased in the Cdc2AF+Wee1-OP11-treated extracts (Figures 5D and 5E, right), in contrast to the abrupt decreases normally seen (Figures 5D and 5E, left). The decrease in Cdc2 activity was accompanied by nuclear-envelope re-formation, suggesting that the extracts were entering interphase. However, although some DNA synthesis could be detected during each subsequent interphase-like period (Figure 5B, right), the extent of DNA synthesis was small compared to that during the first interphase (Figure 5B, right) or during any of the interphases of the buffer-treated extracts (Figure 5B, left). Overall, the Cdc2AF+Wee1-OP11-treated extracts displayed two or three gradual cycles of Cdc2 activation and inactivation (Figures 5D and 5E, right), exhibited gradual mitotic entry and exit with unusual intermediate nuclear morphologies (Figure 5C), and showed little DNA synthesis after the first mitosis (Figure 5B, right). These findings underscore the importance of positive feedback in the production of qualitatively normal cell-cycle oscillations.

Positive Feedback Is Required to Properly Activate the Negative-Feedback Loop

In extracts supplemented with either Cdc2AF (Figure 2F) or with Cdc2AF plus Wee1-OP11 (Figure 5), the postmitotic deactivation of Cdc2 appeared to be sluggish and incomplete. In control extracts (Figure 5D, left) and Cdc2wt-treated extracts (Figure 2E, left), the inactivation of Cdc2 was generally complete within 10 min. In contrast, in the Cdc2AF-treated extracts (Figure 2E, right) and Cdc2AF/Wee1-OP11-treated extracts (Figure 5D, right), the inactivation of Cdc2 often took place over 20–30 min. This suggested that positive feedback in the activation of Cdc2 might be essential for normal mitotic activation of the APC.

To test this hypothesis, we measured the initial rate of cyclin degradation as a function of time in control extracts and extracts treated with Cdc2AF and Wee1-OP11 (Figure 6). In buffer-treated extracts, cyclin destruction was initially slow, increased sharply as the extracts entered mitosis, and returned to low levels immediately following this peak (Figure 6B, left). In contrast, cyclin destruction increased gradually in the extracts treated with Cdc2AF and Wee1-OP11 and never reached the high levels seen in the buffer-treated ex-

(B) DNA replication. DNA synthesis was measured for extracts treated with buffer, 200 nM Cdc2wt plus 20 nM Wee1-OP11, or 200 nM Cdc2AF plus 20 nM Wee1-OP11. Data are from one (left) or two (center, right) independent experiments.

(C) Sperm-chromatin morphology. Sperm chromatin was added to extracts; aliquots were taken at various times and stained with DAPI. Time points containing mitotic nuclei are denoted by solid bars; those containing both mitotic and interphase nuclei are denoted by hatched bars. These photomicrographs correspond to experiment 2 in (A) and (D).

(D) Time course of histone H1 kinase activities for extracts treated with 200 nM Cdc2wt or 200 nM Cdc2AF. Data are taken from two (middle) or three (left, right) independent experiments.

(E) Pooled H1 kinase data. The time courses from individual experiments were rescaled to make the third peak of Cdc2 activation in the buffer-treated extracts occur at t = 3.0 units. The rescaled data were taken together and expressed as running averages, with two (middle) or three (left, right) data points per average. Data are plotted as means ± SEM.

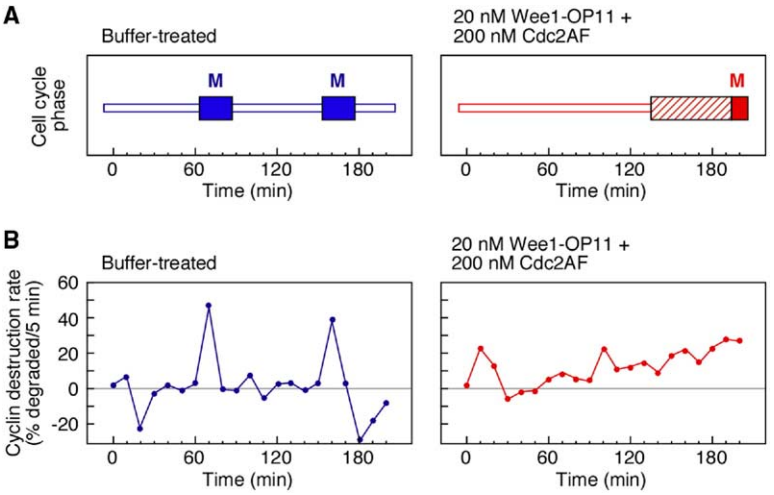

Figure 6. Cyclin Destruction in Control Extracts and Extracts Treated with Cdc2AF and Wee1-OP11

Cycling extracts were supplemented with Cdc2AF (200 nM) and Wee1-OP11 (20 nM). Aliquots were taken for sperm-chromatin morphology (A) and for cyclin-destruction assays (B).

tracts (Figure 6B, right). These results suggest that the APC normally filters out the low levels of Cdc2 activity that accumulate prior to mitosis (hence the low levels of cyclin degradation seen during the interphases in Figure 6B, left) and then converts the switch-like mitotic activation of Cdc2 into switch-like activation of the APC (Figure 6B, left). However, APC activation becomes more temporally graded and incomplete if positive feedback in Cdc2 activation is compromised (Figure 6B, right). Therefore, positive feedback in Cdc2 activation is required to prevent the APC from settling into an intermediate activity state.

The Cdc2-Cyclin Phase Plot of Extracts Treated with Cdc2AF and Wee1-OP11

Finally, we examined the dynamical relationship between cyclin levels and Cdc2 activity in extracts treated with Cdc2AF and Wee1-OP11 to compromise the positive-feedback loops. As shown in Figure 7A, cyclin levels rose approximately linearly over the first 30 min, rose more gradually over the next 60 min, and then began to fall gradually. This is consistent with the previous finding that the rate of cyclin degradation increased linearly over time in extracts treated with Cdc2AF and Wee1-OP11 (Figure 6B, right). Cdc2 activity rose and fell gradually as well, lagging somewhat behind the cyclin levels (Figure 7A). In the phase-plot representation, the Cdc2 activities and cyclin levels lie on a narrow loop, similar to the loops modeled in Figures 1O and 1T, with the upstroke of the loop almost superimposable on the downstroke (Figure 7B). The narrowness of the loop probably partly reflects the fact that the cycles are slow in the Cdc2AF+Wee1-OP11-treated extracts, reducing the "momentum" of the phase-plane orbit (compare Figures 1C and 1E; see also Figure S2), as well as the collapse of the steady-state hysteresis loop that is expected in the Cdc2AF+Wee1-OP11-treated extracts. Thus, compromising positive feedback by forcing the extract to run off Cdc2AF converts the normal, high-amplitude limit cycles into a very low-amplitude cycle incapable of supporting distinct S and M phases.

Discussion

Here we have investigated the role of two subcircuits of the Cdc2/APC system—the Cdc2-Wee1/Myt1 and Cdc2-Cdc25 feedback loops, which on their own function as a bistable switch—in the dynamical behavior of the complete Cdc2/APC system in *Xenopus* egg extracts. Through computational studies, we show that, in the limit of slow cyclin synthesis and destruction, a hysteretic, bistable steady-state response is required for an oscillatory dynamical response (Figures 1B–1U). However, at realistic rates of cyclin synthesis and destruction, the requirement for bistability is relaxed (Figures 1B–1U; Figure S2); overshoots of the hysteretic, steady-state stimulus/response loop can allow oscillations to persist in the absence of bistability, and experimental studies show that such overshoots are in fact present in cycling *Xenopus* egg extracts (Figure 1W). Nevertheless, when the positive-feedback loops are short-circuited experimentally by the addition of modest concentrations of Cdc2AF alone (Figures 2 and 3) or Cdc2AF plus Wee1-OP11 (Figures 5–7), oscillations become severely compromised. The activation of Cdc2 becomes more gradual and less explosive (Figures 2 and 5). This in turn compromises the activation of cyclin destruction; instead of turning on abruptly for a brief period of time, cyclin destruction gradually rises to an intermediate level (Figure 6). This makes the postmitotic inactivation of Cdc2 sluggish and incomplete (Figures 2 and 5), which decreases the duration of the next interphase (Figure 2), resulting in compromised DNA synthesis (Figure 3). Overall, the repetitive spikes of Cdc2 and APC activities normally seen in cycling extracts are converted to damped oscillations centered on intermediate levels of Cdc2 and APC activity (Figures 2, 5, and 6). Thus, the positive-feedback loops in the Cdc2/APC system appear to be essential to the proper running of the cell-cycle oscillator.

We also found that extracts treated with Cdc2AF or Cdc2AF plus Wee1-OP11 often yielded a few time points where interphase and M phase nuclei coexisted (Figures 2 and 5). This might be a simple consequence of the more gradual transition into M phase, but it might

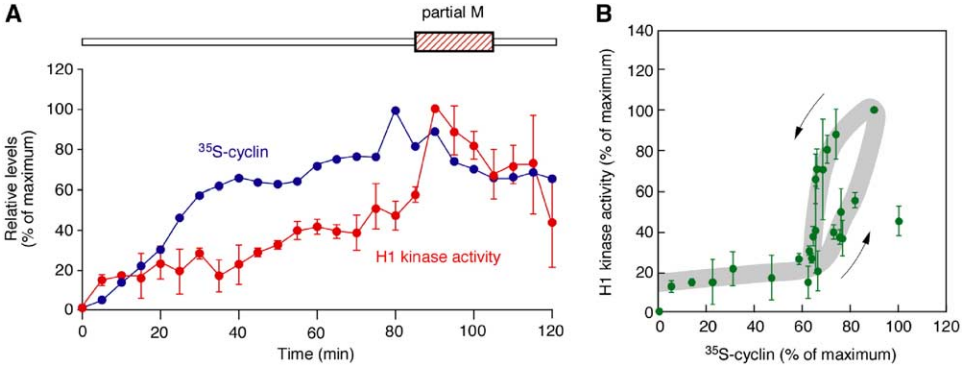

Figure 7. The Dynamical Relationship between Cyclin Levels and Cdc2 Activity in Extracts Treated with Cdc2AF and Wee1-OP11

[^{35}S]methionine was added to a cycling *Xenopus* egg extract supplemented with Cdc2AF (200 nM) and Wee1-OP11 (20 nM), and aliquots were taken every 5 min to determine relative levels of cyclins and Cdc2 H1 kinase activity. Additional aliquots were taken every 10 min to assess the morphology of added sperm chromatin by DAPI staining and epifluorescence microscopy.

(A) Time course of morphological changes (single determinations), cyclin levels (single determinations), and H1 kinase activities (duplicate determinations; quantitated data are shown as means ± SEM). The hatched bar indicates time points with both interphase and M phase nuclei.

(B) Phase plot of the relationship between cyclin levels and Cdc2 activity. In this representation, the data points lie on a narrow loop (drawn in gray).

also reflect some lack of spatial coherence in the activation of Cdc2 in extracts where positive feedback is compromised. Any such spatial incoherence could contribute to the observed damping of the Cdc2 oscillations. Under some circumstances, activity waves can propagate rapidly through a medium that contains a bistable system (Goldbeter, 1996; Hodgkin and Huxley, 1952; Reynolds et al., 2003). It would be of interest to experimentally test the idea that bistability might help to spatially synchronize the process of mitosis.

Our results may help explain a puzzling result from Rudner and Murray on mitotic exit in budding yeast. They found that a nonphosphorylatable form of yeast Cdk1, Cdc28VF, was defective for mitotic activation of APC^{Cdc20} (Rudner and Murray, 2000). This seemed surprising in light of the fact that the specific activity of Cdc28VF was only slightly reduced compared to wild-type Cdc28, and it raised the possibility that the T18V and Y19F mutations might affect the ability of Cdc28 to phosphorylate some substrates but not others. Our finding that Cdc2AF compromises the activation of cyclin destruction in egg extracts, where mitotic cyclin destruction is due to APC^{Cdc20} (Lorca et al., 1998), suggests that perhaps altered dynamics of Cdk1 activation—that is, a lack of normal abruptness in Cdk1 activation—results in gradual and incomplete activation of APC^{Cdc20} in both systems.

In physics and engineering, the best-studied oscillators are probably harmonic oscillators, where the amplitude of the oscillator depends upon initial conditions, and limit-cycle oscillators, where the oscillator eventually finds the same phase-plane orbit irrespective of initial conditions. In biology, two specific types of limit-cycle oscillators are thought to be of particular importance. The first can be termed a negative-feedback oscillator. Oscillators of this class contain a single negative-feedback loop that must consist of at least three components (or, more accurately, the system of differential equations describing the loop must contain at least three independent variables) to keep the oscillator from converging to a stable steady state (Griffith, 1968). Their outputs are typically fairly sinusoidal, and the overall control of the oscillator is shared by all components of the loop. Elowitz's repressilator (Elowitz and Leibler, 2000) is an example of a negative-feedback, limit-cycle oscillator. Other examples include Goldbeter's model of cell-cycle oscillations (Goldbeter, 1991), Igoshin et al.'s model of myxobacterial rippling (Igoshin et al., 2004), and Goodwin's model of circadian rhythms (Goodwin, 1965; Ruoff et al., 1999). The second class relies on positive feedback as well as negative feedback to function. The outputs of these oscillators are typically burst-like or pulsatile rather than sinusoidal. Furthermore, for most of the cycle, the control of the oscillations resides exclusively in a slowly integrated "leak" (analogous to the charging of a capacitor), and, for only a brief period, the oscillations are controlled by the firing of the positive- and negative-feedback loops (analogous to the abrupt discharging of a capacitor) (Nave, 2005). Examples include the Hodgkin-Huxley model of repetitive action potentials (Hodgkin and Huxley, 1952), most models of intracellular calcium oscillations (Berridge, 2001; Meyer and Stryer, 1990), our model (Supplemental Data) and the Novak-Tyson model (Marlovits et al., 1998; Novak and Tyson, 1993) of Cdk oscillations, and some models of circadian rhythms (Reppert and Weaver, 2002; Tyson et al., 1999). The present results strongly argue that the Cdc2/APC system in *Xenopus* egg extracts does in fact rely upon positive feedback as well as negative feedback.

An important question then is why nature appears to have repeatedly made use of this particular oscillator design rather than a straight negative-feedback oscillator or any of the myriad types of more complex circuits that can oscillate. One possibility is that the switch-like behavior of the circuit came first and the oscillatory behavior came later. Perhaps mitosis was originally controlled by an enzyme that produced a graded re-

sponse; then, cooperativity or ultrasensitivity evolved, making the response more decisive; then, positive feedback was added, turning the switch-like ultrasensitive response into a still-more-decisive bistable response; and, finally, a slow negative-feedback loop was added to allow the system to reset periodically. The persistence of a bistable trigger in the present cell-cycle oscillator might be an evolutionary holdover, a consequence of the order in which the various subcircuits of the whole system appeared.

The alternative is that a positive-feedback trigger gives oscillators some fundamental design advantage. One possible advantage is suggested by the computations shown in Figure 1: a relaxation oscillator will still function when the driving force for the oscillator (cyclin synthesis, in the case of the cell cycle) is markedly slowed, whereas a negative-feedback oscillator would not. Thus, with a relaxation oscillator, the same basic machinery could be used to drive either rapid cell cycles (such as those in *Xenopus* and *Drosophila* embryos) or much slower cycles (such as those in somatic cells). Another advantage of this type of oscillator arises out of its integrate-and-fire character. Noise in the number of cyclin transcripts per cell or the rate of cyclin synthesis should have a relatively small effect on the rate of oscillations since it is the amount of accumulated cyclin (essentially, the integral of the rate of cyclin synthesis) rather than the rate of cyclin synthesis per se that determines the timing of the cycle (cf. Barkai and Leibler, 2000). There are many other possibilities for why oscillators triggered by positive feedback might be particularly robust, evolvable, or suitable for biological applications. It remains an intriguing challenge for computational and theoretical biologists to articulate these ideas and for synthetic and analytical systems biologists to test them.

Experimental Procedures

Details about cloning, mutagenesis, purification of recombinant proteins, and in vitro transcription/translation can be found in the Supplemental Data.

Xenopus Egg-Extract Preparation, Functional Assays of Recombinant Proteins, and Cdc2 Kinase Assays

Interphase cytosol and demembranated sperm chromatin were prepared as described previously (Murray, 1991). Steady-state-response experiments using interphase extracts were performed in duplicate. Recombinant Wee1 (20 nM) was added to interphase extract and incubated for 45 min at 22°C. Each reaction was aliquoted, mixed with increasing concentrations of nondegradable cyclin B1 protein, and incubated for 2 hr at 22°C. Samples were frozen on dry ice for later use in kinase assays. The activities of recombinant Cdc2 isoforms were tested by treating interphase extract with 200 nM Cdc2wt or Cdc2AF for 30 min at 22°C, then incubating these mixtures with increasing concentrations of Δ65-cyclin B1 for an additional 2 hr. Samples of extract were removed and frozen on dry ice for subsequent kinase assays.

Cycling extracts used in time-course experiments were prepared from dejellied eggs treated for 2 min with 0.5 μg/ml calcium ionophore A23187 (Sigma-Aldrich, St. Louis) and were mixed with recombinant proteins, *Xenopus cyclin B1* mRNA, or protein buffer as indicated and were then incubated at 22°C. Samples of egg extract were removed at various intervals and frozen on dry ice for subsequent kinase assays.

Cyclin-degradation assays were done by mixing 2 μl of in vitro-translated, ^{35}S-labeled cyclin B1 with 4 μl of egg extract, incubating the samples for 5 min at 22°C, and stopping the reactions with protein sample buffer. Cyclin B1 levels were monitored during the Cdc2-cyclin B phase-plot experiments by labeling cycling egg extracts with 0.3 μCi/μl of [^{35}S]methionine (PerkinElmer Life Sciences, Boston) and freezing 8 μl samples on dry ice during the indicated time intervals. Samples were thawed with ice-cold EB buffer (80 mM β-glycerophosphate, 20 mM EGTA, and 15 mM $MgCl_2$ [pH 7.3]) and precipitating Cdc2/^{35}S-labeled cyclin complexes using p13 agarose. Samples for histone H1 kinase assays and cyclin-degradation assays, as well as p13-precipitated proteins, were electrophoresed through 12.5% Criterion gels (Bio-Rad, Hercules, California) and transferred onto PVDF (Millipore, Bedford, Massachusetts). ^{32}P-labeled histone was detected by autoradiography using Biomax MR film (Kodak, Rochester, New York) and was also quantified by phosphorimaging (Amersham Pharmacia Biotech, Piscataway, New Jersey).

To assess nuclear morphology and nuclear-envelope breakdown (NEBD) as well as perform DNA-replication assays (see below), demembranated sperm chromatin was added to extracts (1000 sperm/μl), then stained with DAPI and analyzed by fluorescence and phase microscopy. Cell-cycle phase was determined by analyzing at least five microscopic fields using a 40× objective. The criteria for M phase entry were condensed chromatin and a lack of a discernable nuclear envelope in at least 90% of the nuclei. The criterion for M phase exit was the reappearance of a smooth nuclear envelope around chromatin. In a few samples, we found both condensed M phase chromatin and large interphase nuclei. These were considered intermediate in cell-cycle state.

DNA-Replication Assays

DNA replication was measured during time-course experiments as described previously (Walter et al., 1997), with minor variations. At 15 min intervals, 5 μl of egg extract was removed and mixed with 1 μl (1 μCi) of [α-^{32}P]dCTP (PerkinElmer Life Sciences) and incubated for 15 min at 22°C, and reactions were stopped by adding 6 μl stop solution. Reactions were treated with 0.83 μg/μl Proteinase K, incubated at 37°C for 60 min, and vortexed, and entire samples were electrophoresed through a 0.8% TAE agarose gel. Following electrophoresis, gels were rinsed in distilled water for 15 min and dried onto 3MM chromatography paper (Whatman International, Maidstone, United Kingdom), and then labeled, replicated chromatin was quantified by phosphorimaging.

Supplemental Data

Supplemental Data include Supplemental Experimental Procedures, Supplemental References, and three figures and can be found with this article online at http://www.cell.com/cgi/content/full/122/4/565/DC1/.

Acknowledgments

We thank Jill Sible and Ian Auckland for suggesting the Wee1-supplementation experiments, Jason Myers for providing *Xenopus* oocyte cDNAs, and members of the Ferrell lab for suggestions and comments on the manuscript. This work was supported by NIH grants R01 GM61276 and T90 DK70090 and a C.F. Aaron Dean's Fellowship.

Received: February 9, 2005
Revised: April 26, 2005
Accepted: June 14, 2005
Published: August 25, 2005

References

Barkai, N., and Leibler, S. (2000). Circadian clocks limited by noise. Nature *403*, 267–268.

Berridge, M.J. (2001). The versatility and complexity of calcium signalling. Novartis Found. Symp. *239*, 52–64. discussion 64–67, 150–159.

Cross, F.R., Archambault, V., Miller, M., and Klovstad, M. (2002).

Testing a mathematical model of the yeast cell cycle. Mol. Biol. Cell *13*, 52–70.

Elowitz, M.B., and Leibler, S. (2000). A synthetic oscillatory network of transcriptional regulators. Nature *403*, 335–338.

Evans, T., Rosenthal, E.T., Youngblom, J., Distel, D., and Hunt, T. (1983). Cyclin: a protein specified by maternal mRNA in sea urchin eggs that is destroyed at each cleavage division. Cell *33*, 389–396.

Ferrell, J.E. (2002). Self-perpetuating states in signal transduction: positive feedback, double-negative feedback and bistability. Curr. Opin. Cell Biol. *14*, 140–148.

Gabrielli, B.G., Roy, L.M., Gautier, J., Philippe, M., and Maller, J.L. (1992). A cdc2-related kinase oscillates in the cell cycle independently of cyclins G2/M and cdc2. J. Biol. Chem. *267*, 1969–1975.

Goldbeter, A. (1991). A minimal cascade model for the mitotic oscillator involving cyclin and cdc2 kinase. Proc. Natl. Acad. Sci. USA *88*, 9107–9111.

Goldbeter, A. (1996). Biochemical Oscillations and Cellular Rhythms (Cambridge: Cambridge University Press).

Goldbeter, A. (2002). Computational approaches to cellular rhythms. Nature *420*, 238–245.

Goodwin, B.C. (1965). Oscillatory behavior in enzymatic control processes. In Advances in Enzyme Regulation, G. Weber, ed. (Oxford: Pergamon), pp. 425–438.

Griffith, J.S. (1968). Mathematics of cellular control processes. I. Negative feedback to one gene. J. Theor. Biol. *20*, 202–208.

Hara, K., Tydeman, P., and Kirschner, M. (1980). A cytoplasmic clock with the same period as the division cycle in Xenopus eggs. Proc. Natl. Acad. Sci. USA *77*, 462–466.

Hartley, R.S., Rempel, R.E., and Maller, J.L. (1996). In vivo regulation of the early embryonic cell cycle in Xenopus. Dev. Biol. *173*, 408–419.

Hershko, A., Ganoth, D., Sudakin, V., Dahan, A., Cohen, L.H., Luca, F.C., Ruderman, J.V., and Eytan, E. (1994). Components of a system that ligates cyclin to ubiquitin and their regulation by the protein kinase cdc2. J. Biol. Chem. *269*, 4940–4946.

Hodgkin, A.L., and Huxley, A.F. (1952). A quantitative description of membrane current and its application to conduction and excitation in nerve. J. Physiol. *117*, 500–544.

Hoffmann, I., Clarke, P.R., Marcote, M.J., Karsenti, E., and Draetta, G. (1993). Phosphorylation and activation of human cdc25-C by cdc2–cyclin B and its involvement in the self-amplification of MPF at mitosis. EMBO J. *12*, 53–63.

Igoshin, O.A., Goldbeter, A., Kaiser, D., and Oster, G. (2004). A biochemical oscillator explains several aspects of Myxococcus xanthus behavior during development. Proc. Natl. Acad. Sci. USA *101*, 15760–15765.

Jin, P., Hardy, S., and Morgan, D.O. (1998). Nuclear localization of cyclin B1 controls mitotic entry after DNA damage. J. Cell Biol. *141*, 875–885.

King, R.W., Peters, J.M., Tugendreich, S., Rolfe, M., Hieter, P., and Kirschner, M.W. (1995). A 20S complex containing CDC27 and CDC16 catalyzes the mitosis-specific conjugation of ubiquitin to cyclin B. Cell *81*, 279–288.

King, R.W., Deshaies, R.J., Peters, J.M., and Kirschner, M.W. (1996). How proteolysis drives the cell cycle. Science *274*, 1652–1659.

Krek, W., and Nigg, E.A. (1991). Mutations of p34cdc2 phosphorylation sites induce premature mitotic events in HeLa cells: evidence for a double block to p34cdc2 kinase activation in vertebrates. EMBO J. *10*, 3331–3341.

Kumagai, A., and Dunphy, W.G. (1992). Regulation of the cdc25 protein during the cell cycle in Xenopus extracts. Cell *70*, 139–151.

Lorca, T., Castro, A., Martinez, A.M., Vigneron, S., Morin, N., Sigrist, S., Lehner, C., Doree, M., and Labbe, J.C. (1998). Fizzy is required for activation of the APC/cyclosome in Xenopus egg extracts. EMBO J. *17*, 3565–3575.

Marlovits, G., Tyson, C.J., Novak, B., and Tyson, J.J. (1998). Modeling M-phase control in Xenopus oocyte extracts: the surveillance mechanism for unreplicated DNA. Biophys. Chem. *72*, 169–184.

McGowan, C.H., and Russell, P. (1995). Cell cycle regulation of human WEE1. EMBO J. *14*, 2166–2175.

Meyer, T., and Stryer, L. (1990). Transient calcium release induced by successive increments of inositol 1,4,5-trisphosphate. Proc. Natl. Acad. Sci. USA *87*, 3841–3845.

Minshull, J., Pines, J., Golsteyn, R., Standart, N., Mackie, S., Colman, A., Blow, J., Ruderman, J.V., Wu, M., and Hunt, T. (1989). The role of cyclin synthesis, modification and destruction in the control of cell division. J. Cell Sci. Suppl. *12*, 77–97.

Minshull, J., Golsteyn, R., Hill, C.S., and Hunt, T. (1990). The A- and B-type cyclin associated cdc2 kinases in Xenopus turn on and off at different times in the cell cycle. EMBO J. *9*, 2865–2875.

Morgan, D.O. (1997). Cyclin-dependent kinases: engines, clocks, and microprocessors. Annu. Rev. Cell Dev. Biol. *13*, 261–291.

Mueller, P.R., Coleman, T.R., and Dunphy, W.G. (1995a). Cell cycle regulation of a Xenopus Wee1-like kinase. Mol. Biol. Cell *6*, 119–134.

Mueller, P.R., Coleman, T.R., Kumagai, A., and Dunphy, W.G. (1995b). Myt1: a membrane-associated inhibitory kinase that phosphorylates Cdc2 on both threonine-14 and tyrosine-15. Science *270*, 86–90.

Murray, A.W. (1991). Cell cycle extracts. Methods Cell Biol. *36*, 581–605.

Murray, A.W., and Kirschner, M.W. (1989a). Cyclin synthesis drives the early embryonic cell cycle. Nature *339*, 275–280.

Murray, A.W., and Kirschner, M.W. (1989b). Dominoes and clocks: the union of two views of the cell cycle. Science *246*, 614–621.

Murray, A.W., Solomon, M.J., and Kirschner, M.W. (1989). The role of cyclin synthesis and degradation in the control of maturation promoting factor activity. Nature *339*, 280–286.

Nave, C.R. (2005). Relaxation Oscillator Concept (http://hyperphysics.phy-astr.gsu.edu/hbase/electronic/relaxo.html).

Norbury, C., Blow, J., and Nurse, P. (1991). Regulatory phosphorylation of the $p34^{cdc2}$ protein kinase in vertebrates. EMBO J. *10*, 3321–3329.

Novak, B., and Tyson, J.J. (1993). Numerical analysis of a comprehensive model of M-phase control in Xenopus oocyte extracts and intact embryos. J. Cell Sci. *106*, 1153–1168.

Pomerening, J.R., Sontag, E.D., and Ferrell, J.E., Jr. (2003). Building a cell cycle oscillator: hysteresis and bistability in the activation of Cdc2. Nat. Cell Biol. *5*, 346–351.

Reppert, S.M., and Weaver, D.R. (2002). Coordination of circadian timing in mammals. Nature *418*, 935–941.

Reynolds, A.R., Tischer, C., Verveer, P.J., Rocks, O., and Bastiaens, P.I. (2003). EGFR activation coupled to inhibition of tyrosine phosphatases causes lateral signal propagation. Nat. Cell Biol. *5*, 447–453.

Rudner, A.D., and Murray, A.W. (2000). Phosphorylation by Cdc28 activates the Cdc20-dependent activity of the anaphase-promoting complex. J. Cell Biol. *149*, 1377–1390.

Ruoff, P., Vinsjevik, M., Monnerjahn, C., and Rensing, L. (1999). The Goodwin oscillator: on the importance of degradation reactions in the circadian clock. J. Biol. Rhythms *14*, 469–479.

Sha, W., Moore, J., Chen, K., Lassaletta, A.D., Yi, C.S., Tyson, J.J., and Sible, J.C. (2003). Hysteresis drives cell-cycle transitions in Xenopus laevis egg extracts. Proc. Natl. Acad. Sci. USA *100*, 975–980.

Solomon, M.J., Glotzer, M., Lee, T.H., Philippe, M., and Kirschner, M.W. (1990). Cyclin activation of $p34^{cdc2}$. Cell *63*, 1013–1024.

Sudakin, V., Ganoth, D., Dahan, A., Heller, H., Hershko, J., Luca, F.C., Ruderman, J.V., and Hershko, A. (1995). The cyclosome, a large complex containing cyclin-selective ubiquitin ligase activity, targets cyclins for destruction at the end of mitosis. Mol. Biol. Cell *6*, 185–197.

Tang, Z., Coleman, T.R., and Dunphy, W.G. (1993). Two distinct mechanisms for negative regulation of the Wee1 protein kinase. EMBO J. *12*, 3427–3436.

Thron, C.D. (1996). A model for a bistable biochemical trigger of mitosis. Biophys. Chem. *57*, 239–251.

Tyson, J.J., Hong, C.I., Thron, C.D., and Novak, B. (1999). A simple model of circadian rhythms based on dimerization and proteolysis of PER and TIM. Biophys. J. *77*, 2411–2417.

Walter, S.A., Guadagno, T.M., and Ferrell, J.E., Jr. (1997). Induction of a G2-phase arrest in *Xenopus* egg extracts by activation of p42 MAP kinase. Mol. Biol. Cell *8*, 2157–2169.

Walter, S.A., Guadagno, S.N., and Ferrell, J.E., Jr. (2000). Activation of Wee1 by p42 MAPK in vitro and in cycling Xenopus egg extracts. Mol. Biol. Cell *11*, 887–896.